Simulation of the lateral movement of NO_3-N in soils following liquid manure injection

B. Assefa and Y. Chen

Department of Biosystems Engineering, University of Manitoba, Winnipeg, Manitoba R3T 5V6, Canada.
**Email: ying_Chen@umanitoba.ca*

Assefa, B. and Chen, Y. 2008. **Simulation of the lateral movement of NO_3-N in soils following liquid manure injection.** Canadian Biosystems Engineering/Le génie des biosystèms au Canada **50**: 2.17–2.26. Understanding manure nitrate-nitrogen (NO_3-N) movement in soil is essential to determine manure placement for efficient use of the NO_3-N in the manure. A two-dimensional model for simulating NO_3-N movement in soils following manure injection was developed. The transport domain for modelling NO_3-N movement was defined by two hypothetical planes midway between centrelines of two consecutive manure bands in the vertical plane. The Hydrus-2D software package was used in computation of Richards flow and convection-dispersion (CDE) solute transport equations. The model was calibrated and validated with previous field data of injecting manure at a tool spacing of 0.9 m and 3.6 litres of manure per meter of manure band. Soil hydraulic and transport parameters were inversely optimised using one set of the field data. The model was validated against another set of the field data. The model results indicated that little manure NO_3-N applied to soil moved laterally beyond 0.20 m from manure band. When compared with the field measurements, the model predicted well the trend of soil NO_3-N distribution in the lateral direction between manure bands; however, underestimations and overestimations were noticed in most cases. The relative errors between the predictions and field measurements ranged from 13.4 to 75.8%. **Keywords:** model, Hydrus-2D, soil, NO_3-N, manure, injection, movement.

La compréhension de la dynamique du mouvement des nitrates (NO_3-N) dans le sol est essentielle à la détermination du placement optimal du lisier de porc dans le sol en relation avec l'utilisation des NO_3-N contenu dans le lisier. Un modèle bidimensionnel prédisant le déplacement des NO_3-N dans le sol suivant l'enfouissement du lisier en bandes (injection) est proposé. L'espace du modèle est défini par deux plans verticaux passant par la ligne centrale de bandes adjacentes de lisier. La plateforme Hydrus-2D a été employée pour résoudre les équations exprimant le mouvement des fluides selon la théorie de Richards et la convection-dispersion des solutés (CDE). Le modèle a été calibré et validé sur la base de données expérimentales obtenues lors d'essais d'injection du lisier avec des enfouisseurs espacés de 0,9 m appliquant 3,6 litres de lisier par mètre de bande. Les paramètres hydrauliques et de transport du modèle ont été optimisés avec une méthode inverse utilisant une partie des données recueillies au champ. Le modèle a ensuite été validé à l'aide de l'autre partie des données. Les résultats suggèrent que peu des NO_3-N du lisier enfouis dans le sol progressent latéralement au-delà de 0,2 m de la bande de lisier. Le modèle représente bien les tendances de distribution des NO_3-N dans le sol entre les bandes de lisier; toutefois, nous avons noté des sous-estimations et surestimations des valeurs dans la plupart des cas. L'erreur entre les valeurs prédites de NO_3-N dans le sol et les données expérimentales varient entre 13,4 et 75,8%. **Mots clés:** modélisation, Hydrus-2D, sol, NO_3-N, lisier, injection, transport.

INTRODUCTION

Increased manure output from more intensified livestock operations has led to an enormous amount of research on manure handling and land application. To date, land application of manure has been considered the most economical method of disposal. Among several application methods, injection has been established as the recommended method of application of liquid manure. In the injection method, manure is placed in the soil in bands. Thus, the uniformity of manure nutrient distribution in soil needs to be addressed. Manure nutrient distribution in soil depends on several factors, among which the lateral movement of manure nutrients between manure bands following manure injection is important. Manure nitrate nitrogen is a nutrient of particular interest in this study.

Nitrate nitrogen movement in soil can be described by the phenomenon of solute transport in soil. Studies of solute transport in the soil using numerical models are becoming more common with the availability of well-established governing flow and transport equations as well as software. The frequently used governing equations are the Richards' equation for water flow and the equilibrium convection-dispersion equation (CDE) or the mobile-immobile equation (MIM) for solute transport (Inoue et al. 2000; Ventrella et al. 2000; Jacques et al. 2002; Abbasi et al. 2004). Some deviations of model predictions from observations of solute concentrations in field soils have been reported when using the CDE, especially in surface soils (Snow et al. 1994; Jacques et al. 1998). In contrast, Abbasi et al. (2003, 2004) reported no differences in results obtained when using CDE and MIM equations.

Hydrus-2D, developed by Simunek et al. (1999), is a software that simulates water and solute movement in two-dimensional (vertical or/and horizontal plane) porous media (Simunek et al. 1999), such as soil. The code numerically solves the Richards equation and the CDE for analyzing water flow and solute transport in saturated/unsaturated media. The software allows for incorporation of sink terms in the flow and transport equations to account for water and nutrient uptakes by plant roots. Several researchers have used Hydrus-2D model to simulate water and solute transport in agricultural soils. For example, Abbasi et al. (2003, 2004) simulated bromide transport in irrigated bare soils using Hydrus-2D. Coquet et al. (2005) used Hydrus-2D to simulate water flow and bromide transport in their study that examined the effect of tillage on the dynamics of water and bromide movement in cultivated soils. Gärdenäs et al. (2005) used Hydrus-2D to model nitrate leaching under various fertigation scenarios. They noted the existence of limited information on soil nitrate distribution.

Numerical modelling of solute transport requires input parameters and specifications of appropriate initial and boundary conditions. Model input parameters, including soil hydraulic and solute transport parameters, are often difficult to measure, particularly at field scale, primarily due to labour and budget constraints (Abbasi et al. 2003). Due to the difficulty, the method of inverse optimisation of those parameters from measured variables of field experiments has been considered a promising approach for determining input parameters. Inverse optimisation is a method of parameter estimation using initial guesstimated parameter values and repeated simulation leading to the best possible set of parameters to reproduce experimentally obtained data (Simunek et al. 1999; Hopmans et al. 2002; Simunek et al. 2002).

Hudrus-2D includes the Levenberg-Marquardt (Marquardt 1963) inverse optimisation procedure. The inverse optimisation can be done simultaneously or sequentially in optimising soil hydraulic and solute transport parameters under imposed proper initial and boundary conditions (Abbasi et al. 2003, 2004; Jacques et al. 2002; Inoue et al. 2000). In the simultaneous approach, both soil hydraulic and transport parameters are optimised at the same time. In the sequential approach they are optimised separately in two steps. In the first step, hydraulic parameters are optimised. In the second step, transport parameters are optimised using the hydraulic parameters obtained in the first step. Simultaneous estimation has been reported to be more beneficial in that it takes advantage of cross-over effects between state parameters (Sun and Yeh 1990) and reduced estimation errors compared with sequential estimation (Mishra and Parker 1989; Simunek et al. 2002). Finally, comparison of model predicted (using optimised parameters) variables with a separate set of experimentally obtained data other than that used in parameter optimisation determines the performance of the model.

Manure NO_3-N can be considered much like other solutes in terms of moving through the soil medium. However, there is little literature on simulation of lateral movement of manure NO_3-N following manure injection. The objectives of this study were: (1) to use Hydrsu-2D software to simulate manure NO_3-N movement away from manure band injected in the soil over a growing season, (2) to inversely optimise soil hydraulic and transport parameters using a set of data collected from field experiments, and (3) to validate the model using a separate data set collected from field experiments.

MODEL EQUATIONS

Hydrus-2D embedded solute transport and flow equations, the required functions of hydraulic parameters, crop water uptake, and nutrient intake. Thus, the main tasks of the model development in this study included defining the transport domain, specifying the initial and boundary conditions, and finding inverse and forward solutions of the equations. These tasks are described later in the paper. The following sections present the transport and flow equations, and plant nutrient uptake and soil hydraulic functions in Hydrus-2D.

Flow equation

In Hydrus-2D, the governing flow equation for two-dimensional isothermal flow of water in the unsaturated soil zone is given by the mixed form of Richard's equation (Simunek et al. 1999; Celia et al. 1990).

$$\frac{\partial \theta}{\partial t} = \frac{\partial}{\partial x_i}\left[K\left(K_{ij}^A \frac{\partial h}{\partial x_j} + K_{ij}^A\right) - S\right] \quad (1)$$

where θ is the volumetric water content ($L^3\ L^{-3}$), K is the unsaturated hydraulic conductivity function ($L\ T^{-1}$), K_{ij}^A are components of a dimensionless anisotropy tensor K^A, h is the pressure head (L), and S is a sink term (T^{-1}) representing the volume of water removed by plant water uptake per unit volume of soil and unit time. Units M, T, L are dimensions of mass, time, and length, respectively. The hydraulic conductivity function in two dimensions is in turn given by:

$$K(h, x, z) = K_s(x, z) K_r(h, x, z) \quad (2)$$

where K_r is the relative hydraulic conductivity, K_s is the saturated hydraulic conductivity ($L\ T^{-1}$), and x and z are lateral and vertical coordinates (L), respectively. The sink term has been defined by Feddes et al. (1978) as follows:

$$S(h) = a(h) S_{\max} \quad (3)$$

where $a(h)$ is a prescribed dimensionless function of the soil pressure head ranging between 0 and 1, and $S_{\max}$ is the potential water uptake rate (T^{-1}).

Transport equation

Hydrus-2D numerically solves the Fickian-based CDE given below for solute transport (Simunek et al. 1999; Gärdenäs et al. 2005).

$$\frac{\partial \theta c}{\partial t} = \frac{\partial}{\partial x_i}\left(\theta D_{ij} \frac{\partial c}{\partial x_j}\right) - \frac{\partial q_i c}{\partial x_i} - NU(c, x_i, t) \quad (4)$$

where, t is time (T), c is the NO_3-N concentration in the liquid phase ($M\ L^{-3}$), x_i and x_j ($i, j = 1,2$) are spatial coordinates (L), D_{ij} are components of dispersion coefficient tensor ($L^2\ T^{-1}$), q_i is the i^{th} component of the volumetric flux density ($L\ T^{-1}$), and NU is the local NO_3-N uptake by plant roots ($M\ L^{-3}\ T^{-1}$). The volumetric flux density (q) to be employed in the above equation determines the nature of transport of dissolved NO_3-N with flowing water. Thus, use of the flow equation is required to calculate the volumetric flux density.

Plant nutrient uptake function

Plant nutrient uptake, *NU*, is the function of time and coordinates. It is related to water uptake in that the nutrient gets taken up by the plants with the water. In Hydrus-2D, *NU* is updated by the following equation at all time:

$$NU(x,z,t) = c(x,z,t)S \qquad (5)$$

Soil hydraulic functions

The closed-form of van Genuchten's (1980) water retention function and Mualem's (1976) conductivity model were employed in Hydrus-2D to calculate moisture content and hydraulic conductivity. The van Genuchten water retention equation is given by:

$$\theta = \frac{\theta_s - \theta_r}{(1 + |\alpha h|^n)^m} \qquad (6)$$

where θ_r is the residual volumetric water content ($L^3\ L^{-3}$), θ_s is the saturated volumetric water content ($L^3\ L^{-3}$), σ and n are retention curve-fitting parameters and $m = 1\text{-}1/n$. Maulem's hydraulic conductivity function is given by:

$$K(h) = K_s S_e^l \lfloor 1 - (1 - S_e^{1/m})^m \rfloor^2 \qquad (7)$$

where $K(h)$ is the unsaturated hydraulic conductivity ($L\ T^{-1}$), K_s is the saturated hydraulic conductivity ($L\ T^{-1}$), m and l are empirical parameters, and l can be assumed to be 0.5 (Mualem 1976). Parameter S_e is a dimensionless relative saturation given by:

$$S_e = \frac{\theta - \theta_r}{\theta_s - \theta_r} \qquad (8)$$

MODEL DEVELOPMENT

Computational domain

Injection of liquid manure creates manure bands as shown in Fig. 1a. The distance between the centres of adjacent manure bands is equal to the injection tool spacing. In the model, the domain for investigating lateral movement of manure NO_3-N in the soil was defined as the cross-sectional area encompassed by two hypothetical planes (Fig. 1b). Each of the hypothetical planes lies midway between centerlines of two consecutive manure bands in the vertical plane. This arrangement results in having a manure band situated midway between the hypothetical planes. The size of the domain was defined by the distance between two hypothetical planes and the depth of interest for soil nutrient movement.

Domain discretisation and manure placement in the domain

The domain can be discretized into a uniform grid mesh (Fig. 2) using the mesh generation feature of Hydrus-2D. The shaded area (A) within the domain represents the cross-section of the manure band placed at the time of injection. The cross-sectional area of the manure band may vary with the manure application rate and injection tool spacing (Rahman et al. 2004). The vertical location of the manure band within the domain mainly depends on the injection depth. It would be rational to consider that the manure band is surrounding a point centered about the injection depth.

Model assumptions

The following assumptions were used in the model development:

1. Manure nutrients from a manure band do not move beyond the hypothetical planes midway between that band and an adjacent manure band.
2. The soil where manure is placed is saturated by liquid manure at the instant of manure injection.
3. The cross-section of manure band is rectangular in shape at the time of manure placement.
4. All NH_4-N in manure is converted to NO_3-N immediately upon manure application.
5. Soil is homogeneous and isotropic; there is no hysteresis effect.
6. Nitrogen dynamics (mineralization/immobilization and denitrification) is neglected.
7. The water table lies far below the domain.

Assumption 1 is based on the fact that manure placed in contiguous manure bands moves towards the middle between the bands with a net effect of no movement past midway between the bands. Assumption 2 is based on the fact that manure is delivered to soil at a "point" which is the outlet of the manure delivery tube behind the injection tool. Assumption 3 was made to match the grid mesh (Fig. 2). Assumption 4 is for the purpose of simplicity. Assumption 5 was based on the assumption stated in Hydrus-2D. The same assumption was also made by Abbasi et al. (2003, 2004) to simulate water and solute transportation. Assumption 6 was for simplicity. The same assumption was made by Gärdenäs et al. (2005) in modelling nitrate leaching using Hydrus-2D. Assumption 7 was based on the fact that manure is placed at the surface layer of soil.

Boundary conditions

At the upper boundary, atmospheric and Cauchy conditions were used (Fig. 2) for solving water flow and solute transport equations, respectively. The atmospheric boundary condition was specified as (Simunek et al. 1999):

$$\left| K\left(K_{ij}^A \frac{\partial h}{\partial x_j} + K_{iz}^A \right) n_i \right| \le E \qquad (9)$$

$$h_A \le h \le h_s \qquad (10)$$

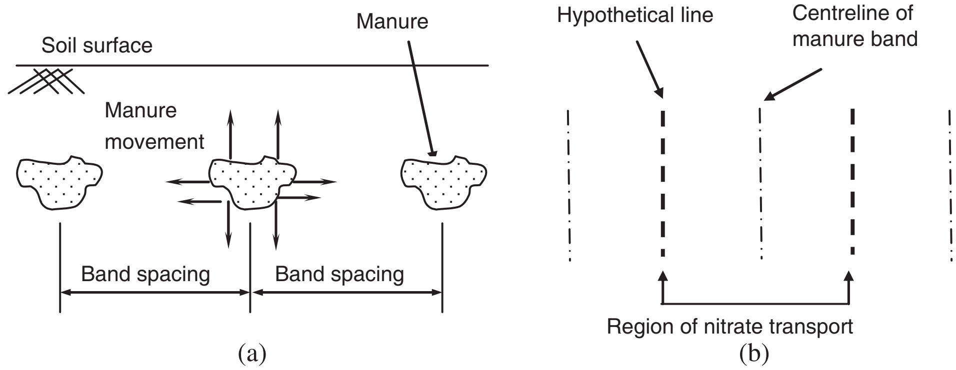

Fig. 1. A schematic diagram showing (a) the cross-section of manure band and hypothesized direction of manure nutrient movement; (b) definition of transport region (top view).

where E is the maximum potential rate of infiltration or evaporation under the current atmospheric conditions, and h_s are minimum and maximum pressure heads allowed under the prevailing soil conditions. While h_s is usually set equal to zero, h_A is determined from the equilibrium conditions between soil water and atmospheric water vapour, with -100 m being the default value in Hydrus-2D. At the bottom of the domain, a free drainage boundary condition is applied to both water flow and solute movement. No flux boundary condition is imposed on the sidewalls of the transport region for both flow and solute transport.

Model inputs

Model inputs include application-related parameters, such as type of crop, injection tool spacing, injection depth, and cross-sectional area of the manure band at the time of injection. Weather-related inputs for the model include precipitation and evapotranspiration. The model inputs related to the transport equation are initial soil NO_3-N concentration, c_i; longitudinal dispersivity, D_L; and transverse dispersivity, D_T. Inputs related to the flow equation are initial soil water content, θ_i; saturated water content, θ_s; residual water content, θ_r; saturated hydraulic conductivity, K_s; empirical constants α and n. The inputs, c_i and θ_i, can be easily measured. The other inputs are more difficult to measure. However, they can be calibrated as described in the following sections.

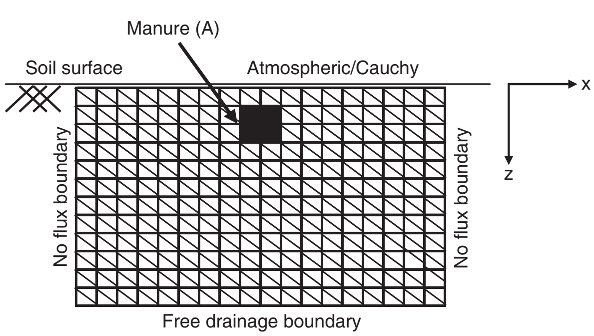

Fig. 2. Cross sectional view of the discretised computational domain in the vertical plane with imposed boundary conditions.

Model calibration theory

In the inverse optimisation procedure, the Rosetta code (Schaap et al. 2001) embedded in Hydrus-2D was used to estimate θ_r,θ_s, and K_s from the soil texture. The remaining two hydraulic parameters (α and n) and the transport parameters (D_L and D_T) were inversely estimated by numerically solving the flow and transport equations with the Levenberg-Marquardt optimisation procedure (Marquardt 1963). The procedure involves minimizing the following objective function (Simunek et al. 1999):

$$\Phi(q,b) = \sum_{j=1}^{m} v_j \sum_{i=1}^{n^*} w_{ij}[q_j(x,z,t_i) - q_j(x,z,t_i,b)]^2 \quad (11)$$

where n^* is number of observations for the j^{th} measurement set (i.e., water content and NO_3-N concentration), $q(x, z, t_i)$ are specific measurements at time t_i, location x, and depth z, q (x, z, t_i, b) are corresponding model predictions for the vector of optimised parameters b (i.e., α, n, D_L and D_T), v_j and w_{ij} are weights associated with a particular measurement set or point, respectively.

MODEL CALIBRATION and VALIDATION

Data source

The data used for model calibration and validation were obtained from the field experiments carried out at the Brandon Research Centre, Brandon, Manitoba, Canada, in the growing seasons of 2003 and 2004 on clay soils (26.0% sand, 21.4% silt, and 52.6% clay). The nitrogen contents and solid content of the liquid swine manure injected are summarised in Table 1. Liquid swine manure was injected using two different types of injection tools (furrowers and discs) and three different injection tool spacings (0.3, 0.6, and 0.9 m). The injection depth was 0.1 m and the manure application rate was 34,000 L/ha. The field plots were seeded to barley following manure injection.

Only the soil NO_3-N data from the largest tool spacing (0.9 m) were used in this study due to the fact that larger spacing between manure bands would have less risk of crossing effects between manure bands. Also, more data points were available for this spacing. The data were

Table 1. Nitrogen content of manure applied (wet basis).

Growing season	Total N ($\mu g\ g^{-1}$)	Organic N ($\mu g\ g^{-1}$)	Ammonium N ($\mu g\ g^{-1}$)	Nitrate and nitrite N ($\mu g\ g^{-1}$)	Solid content (%)
2003	2.9	0.6	2.3	0.1	2.1
2004	3.5	0.4	3.0	0.1	1.6

averaged over the two types of tools due to the small differences between the two types of tools. Soil NO_3-N concentrations were measured three times over each growing season. Collections of soil samples were done at 0, 0.15, 0.30, and 0.45 m from manure band and two depth ranges (0–0.3 and 0.3–0.6 m). The manure application rate, 34,000 L/ha, was equivalent to 3.6 L/m of manure band. The data used for the initial levels of soil NO_3-N and soil water content are listed in Table 2. More detailed description of the experiment, including methods of nutrient analysis can be found in Assefa et al. (2006).

Meteorological data during the growing seasons were obtained from Brandon Research Centre located within 1 km of the site. Crop evapotranspiration was estimated using FAO Penman-Monteith method (Richard et al. 1998). The estimated crop evapotranspiration (1.7 mm d^{-1}) and daily precipitation data (Fig. 3) obtained from the weather station were used as the atmospheric boundary conditions of the model.

Inputs for calibration and validation

For calibration, the model was run with the data source obtained in 2004 using the aforementioned inverse optimisation theory. For validation, the model was run with the 2003 data. Both calibration and validation were performed using the following input values.

The width of the domain was equal to the tool spacing, 0.9 m wide, and the depth of the domain was 0.6 m, which was the depth range of the measurements. Using the mesh generation feature of Hydrus-2D, the domain (Fig. 2) was discretised into a uniform 0.05 m grid mesh resulting in 432 triangular elements and 247 nodes. The Galerkin finite element space weighting scheme was used to generate the mesh, while the Crank-Nicholson time weighting scheme was used for time discretisation (Simunek et al. 1999). Since barley was not listed in Hydrus-2D, "wheat" was selected for the simulation. The cross-sectional area of the manure band was approximated to an area of 0.1×0.1 m, which was two times the diameter (0.05 m) of the manure delivery tube, considering the possibility of manure redistribution after being placed in the soil. The cross-section of the manure band was centred at the injection depth (0.1 m). Initial soil water contents and NO_3-N concentrations in Table 2 were used as the initial conditions. Precipitation data were those shown in Fig. 3. The soil NO_3-N concentrations following manure injection were those measured at varying positions (0, 0.15, 0.30, and 0.45 m) from the centerline of the selected manure band at 0–0.3 and 0.3–0.6 m depths and at different times over the growing seasons.

RESULTS and DISCUSSION

Model calibration

Inverse optimisation was performed both sequentially and simultaneously. The simultaneous approach yielded better results and it was used for calibration. In the optimisation process, three of the hydraulic properties (θ_r, θ_s and K_s) were kept constant at their Rosetta predicted values which were 0.09 $m^3\ m^{-3}$, 0.47 $m^3\ m^{-3}$, and 160.7 mm d^{-1}, respectively. Two hydraulic (α and n) and two transport (D_L and D_T) parameters were inversely optimised from measured soil water contents and NO_3-N concentrations. The model was run several times using different initial estimates of parameters to match the data with model outputs of soil NO_3-N concentrations. Of all the results from the various model runs, the best match between the measured NO_3-N concentration and the corresponding model outputs is presented in Figs. 4 and 5. In most cases, the model outputs of the soil NO_3-N concentration matched the measurements reasonably well, except for only one lateral location (0.15 m) at the 0–0.3 m depth (Fig. 4b) and one location (at manure band) at the 0.3–0.6 m depth (Fig. 5a). For these two locations, the values from the model predictions were higher than those from the field measurements.

The model parameters corresponding to the above calibration results were taken as the optimal model parameters. The optimised value (0.023 mm^{-1}) of α was similar to that estimated with Rosetta (Schaap et al. 2001)

Table 2. Measured initial soil water content (θ_i) and NO_3-N concentrations (c_i).

Growing season	θ_i ($m^3\ m^{-3}$) Entire domain	θ_i ($m^3\ m^{-3}$) Manure band	c_i ($\mu g\ g^{-1}$) Entire domain 0–0.3 m depth	c_i ($\mu g\ g^{-1}$) Entire domain 03–0.6 m depth	c_i ($\mu g\ g^{-1}$) Manure band*
2003	0.27	0.47	14	11	50
2004	0.29	0.47	14	11	61

*Values are the sum total of the initial concentrations in the soil and manure at 100 mm depth.

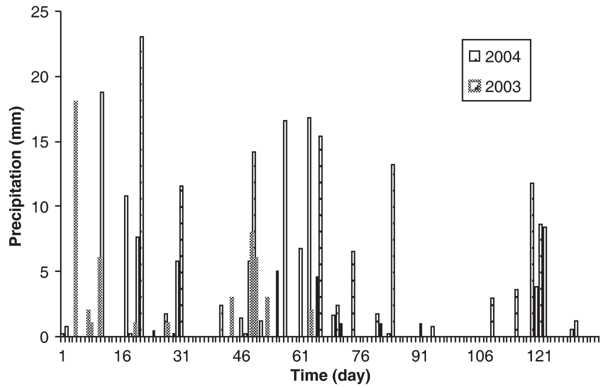

Fig. 3. Precipitation data over the growing seasons of 2003 and 2004.

and the optimised value (2.0) of parameter n as the same as that assumed by van Genuchten (1980). Optimised values (132.5 and 0.1 mm) of D_L and D_T were different from those assumed by Gärdenäs et al. (2005) and Coquet et al. (2005), but within the range of the values reported by Abbasi et al. (2004).

Model validation

The model was run using the optimised soil hydraulic and transport parameters. The results are discussed below in relation to NO_3-N distributions both laterally and over time. Model predictions of NO_3-N concentrations were compared with field measurements in 2003. The agreement between predictions and measurements was evaluated by relative error:

$$RE = \frac{100}{m} \sum_{i=1}^{m} \frac{|M_i - O_i|}{M_i} \qquad (12)$$

where RE is relative error (%); m is number of data points, M_i is the i^{th} measurement, and O_i is the i^{th} model output.

Lateral distribution of NO_3-N in soil The prediction results showed that the soil NO_3-N concentration at the 0-0.3 m depth decreased with the lateral position from the centreline of manure band and, beyond a certain lateral distance, there were no or few changes in NO_3-N (Fig. 6). This means that movement of the soil NO_3-N was limited to a certain lateral position. For example, the lateral distribution of NO_3-N predicted for day 21 after the manure injection was within 0.15 m of the centre of the manure band (Fig. 6a); the lateral distribution of NO_3-N spread over a greater lateral distance (within 0.20 m from the manure band) while going from day 21 to day 42 (Fig. 6b) and day 63 (Fig. 6c). Discrepancies were observed when compared with model predictions to measurements. The model underestimated the soil NO_3-N with R_e from 13.4 to 39.5%. The measurements of NO_3-N showed a continuously decreasing trend over the entire lateral distance of 0.45 m on days 21 and 63 (Fig. 6a, c), while the model predictions seemed to be more sensitive over a distance of 0.15 m and less sensitive further away. At the deeper soil layer (0.3–0.6 m), predictions had similar trends to those at the 0–0.3 m depth (Fig. 7a, b, c). the soil NO_3-N movement was also limited to 0.2 m laterally. Both underestimations and over estimations were observed for the model at this depth range. In general, a better agreement between model predictions and measurements was observed at the 0.15 m lateral distance and greater, compared with the data for the 0–0.3 m depth. The high values (25.3 to 52.7%) of R_e between predictions and measurements were due to the great discrepancies at the 0 m lateral distance (at manure band).

Both predictions and measurements showed limited lateral distributions of soil NO_3-N after manure injection,

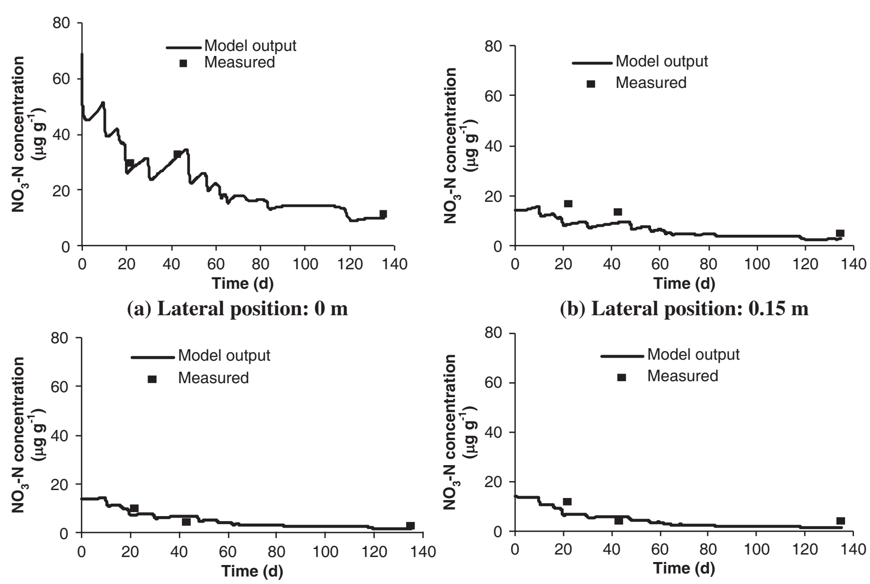

Fig. 4. Model calibration – soil NO_3-N over time at 0–0.3 m depth predicted and measured in 2004.

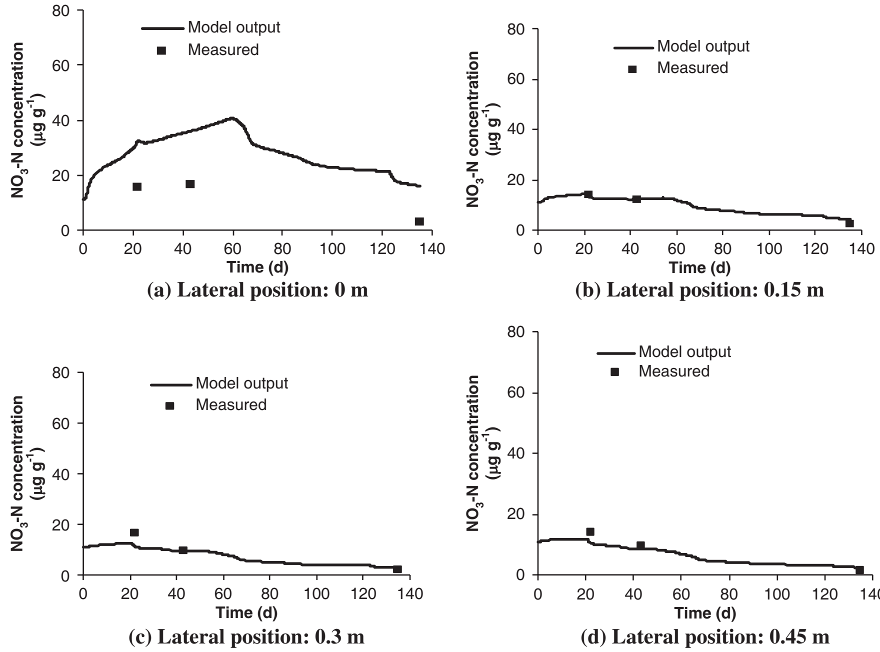

Fig. 5. Model calibration – soil NO_3-N over time at 0.3–0.6 m depth predicted and measured in 2004.

implying that injection of manure in smaller volume at narrower spacing is advantageous over that at wider spacing, in terms of NO_3-N availability. This is in agreement with better plant performance reported by Assefa et al. (2006) when liquid manure was injected at 0.3 m spacing than at 0.9 m spacing.

Nitrate-nitrogen concentration over time

At the 0–0.3 m depth, the general trend of the model prediction was that soil NO_3-N concentration decreased over time for all lateral distances (Fig. 8a, b, c, d). This trend was more obvious at the 0 m lateral distance (manure band) (Fig. 8a). In general, the model underestimated the soil NO_3-N concentrations at all times and lateral distances when compared with the measurements; the model predictions had great discrepancies as demonstrated by the RE values of 29.6 to 47.2%. At this soil depth range, the model performed the best for day 42, followed by day 63 and then day 21. In contrast to the 0–0.3 m depth, the 0.3–0.6 m depth had the lowest predicted values of soil NO_3-N concentration (Fig. 9a); the soil NO_3-N concentrations increased over the lateral distance of approximately 0.1 m and then became constant. This trend was unexpected. There was almost no precipitation between day 10 and day 40; thus, the NO_3-N might have moved upwards due to moisture gradient. At the 0 m lateral distance, the predicted values were lower than those measured at all times, and the RE was very high (75.8%) (Fig. 9a); at the other lateral distances, mixed results were obtained (Fig. 9b, c, d). At the 0.15 and 0.3 m distances, the model performed better and the RE values were under 20%.

The aforementioned findings are consistent with those of Abbasi et al. (2004), who reported mixed results (i.e., underestimation and overestimation of bromide concentrations). They attributed the discrepancies to insufficient data used in their optimization procedure of transport parameters estimation. From results of a study of bromide and nitrate movement through unsaturated soil columns, Clay et al. (2004) concluded that use of bromide for estimating nitrate leaching could lead to an overestimation of 25%. Point measurements yielding poor representation of solute transport at the field scale (Tsang et al. 1996) can also contribute to disagreements between measured and

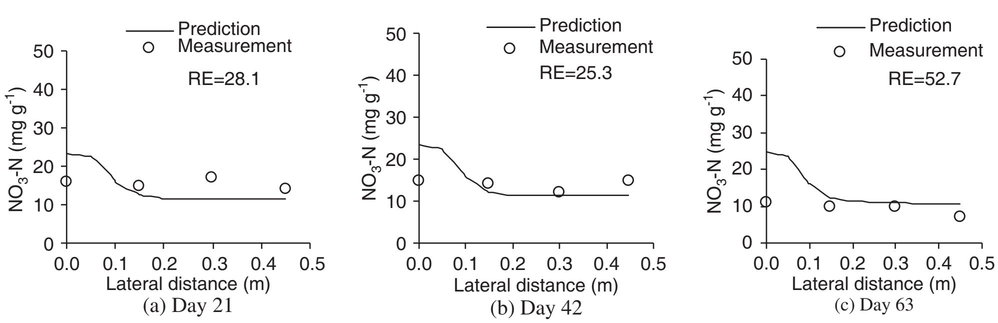

Fig. 6. Soil NO_3-N for different lateral positions – concentrations at the 0–0.3 m depth predicted and measured in 2003.

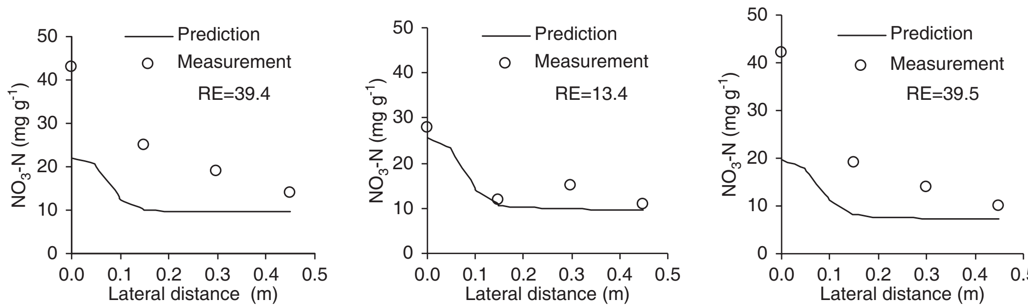

(a) Day 21 (b) Day 42 (c) Day 63

Fig. 7. Soil NO_3-N for different lateral positions concentrations at the 0.3–0.6 m depth predicted and measured in 2003.

predicted values. For example, Ritsema and Dekker (1996) reported underestimation of chemical fluxes attributed to point measurements. According to Xiang et al. (1992) considerable uncertainties exist with point measurements caused by human, instrumental, and hydrological errors. The disagreement between the measured and predicted results may be further explained by the highly variable nature of soil properties and soil nutrient concentrations.

CONCLUSIONS

Hydrus-2D was successfully used in simulating the lateral movement of manure NO_3-N in soil between manure bands following liquid manure injection. The simulation process enhanced the understanding of manure placement and the subsequent movement of the manure nutrients in soil. The model developed allows for simulations of different injection tool spacings and injection depths, as well as different initial manure and soil conditions. Thus, the model has wide applicability for liquid manure injection.

Some model parameters, when not available, can be inversely optimised (calibrated) with good matches between field measurements and the model outputs of soil NO_3-N concentration. Based on the results of the model prediction, it was noticed that little manure NO_3-N applied to soil for crop production moved laterally beyond 0.20 m from the manure band. This evidence implies that swine liquid manure injection is best done at injection tool spacings smaller than 0.40 m to minimize uneven nutrient distribution in soil. The model results on the soil NO_3-N lateral distribution showed trends similar to field measurements, in which the soil NO_3-N decreases further away from the manure band. However, the model results exhibited great discrepancies when compared with the field measurements. Relative errors ranged from 13.4 to 52.7% when predicting lateral NO_3-N distribution and from 14.7 to 75.8% when predicting NO_3-N concentration over the growing season. The occurrences of some underestimations and overestimations may be indicative of the importance of soils' spatial variability and nitrogen dynamics.

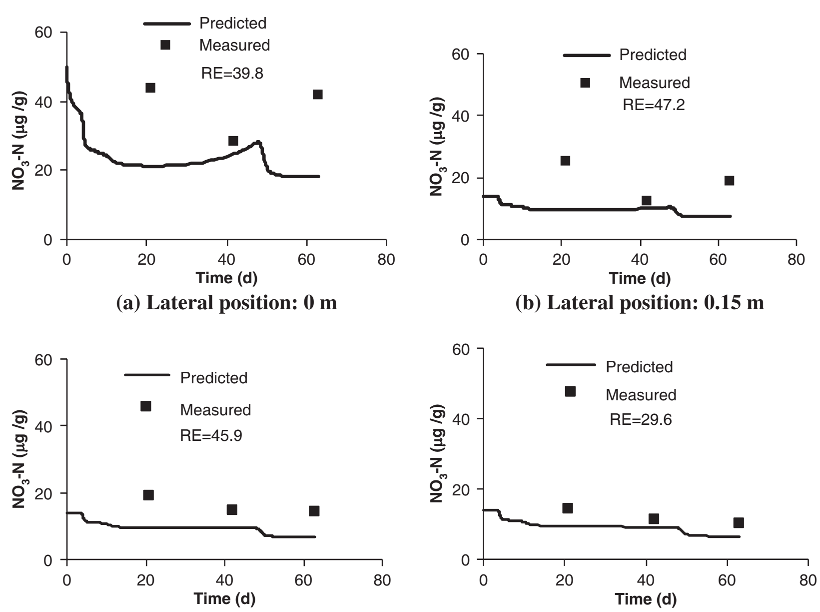

(a) Lateral position: 0 m **(b) Lateral position: 0.15 m**

(c) Lateral position: 0.3 m **(d) Lateral position: 0.45 m**

Fig. 8. Model validation – soil NO_3-N over time at 0–0.3 m depth predicted and measured in 2003.

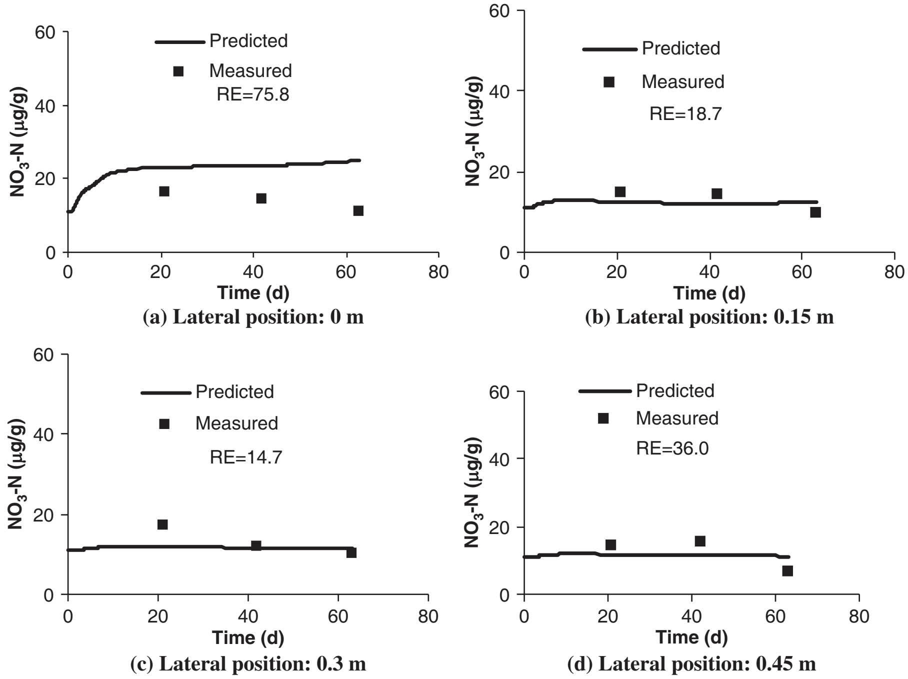

Fig. 9. Model validation – soil NO_3-N over time at 0.3–0.6 m depth predicted and measured in 2003.

It must be emphasized that several assumptions were made in the model development process. The calibration and validation of the model were done using only a clay soil. Also, there were no data for time less than 20 days after manure injection. Further validations of the model may be needed when the model is applied to other situations. Considering nitrogen dynamics, including accurate measurements of some soil hydraulic properties, such as hydraulic conductivity and saturated water content at the field scale, may further improve the model performance.

ACKNOWLEDGEMENT

The financial support from the Natural Sciences and Engineering Research Council of Canada (NSERC) is gratefully acknowledged.

REFERENCES

Abbasi, F., J. Feyen and M.Th. van Genuchten. 2004. Two-dimensional simulation of water flow and solute transport below furrows: Model calibration and validation. *Journal of Hydrology* 290: 63–79.

Abbasi, F., J. Simunek, J. Feyen, M.Th. van Genuchten and P.J. Shouse. 2003. Simultaneous inverse estimation of soil hydraulic and solute transport parameters from transient field experiments: Homogeneous soil. *Transactions of the ASAE* 46: 1085–1095.

Assefa, B.A., Y. Chen, K. Buckley and W. Akinremi. 2006. Effects of manure injection type and tool spacing on soil nutrient levels and spring barley performance. *Canadian Biosystems Engineering* 48: 2.45–2.54.

Celia, M.A., E.T. Bouloutas and R.L. Zarba. 1990. A general mass-conservative numerical solution of the unsaturated flow equation. *Water Resources Research* 26: 1483–1496.

Clay, D.E., Z. Zheng, Z. Liu, S.A. Clay and T.P. Trooien. 2004. Bromide and nitrate movement through undisturbed soil columns. *Journal of Environmental Quality* 33: 338–342.

Coquet, Y., J. Simunek, C. Coutadeur, M.Th. van Genutchten, V. Pot and J. Roger-Estrade. 2005. Water and solute transport in cultivated silt loam soil: 2. Numerical analysis. *Vadose Zone Journal* 4: 587–601.

Feddes, R.A., P.J. Kowalik and H. Zaradny. 1978. Simulation of field water use and crop yield. Simulation monographs. Wageningen, the Netherlands. In *The Hydrus2D software package for simulating two-dimensional movement of water, heat and multiple solutes in variably saturated media, version 2.0*.

Gärdenäs, A.I., J.W. Hopmans, B.R. Hanson and J. Simunek. 2005. Two-dimensional modeling of nitrate leaching for various fertigation scenarios under micro-irrigation. *Agricultural Water Management* 74: 219–242.

Hopmans, J.W., J. Simunek, N. Romano and W. Durner. 2002. Inverse Methods. In *Methods of Soil Analysis: Part 4. Physical Methods*, eds. J.H. Dane and G.C. Topp, 963–1008. Madison, WI: Soil Science Society of America.

Inoue, M., J. Simunek, S. Shiozawa and J.W. Hopmans. 2000. Simultaneous estimation of soil hydraulic and solute transport parameters from transient infiltration experiments. *Advances in Water Resource* 23: 677–688.

Jacques, D., J. Simunek, A. Timmerman and J. Feyen. 2002. Calibration of Richards' and CDEs to field-scale water flow and solute transport under rainfall conditions. *Journal of Hydrology* 259: 15–31.

Jacques, D., J.D. Kim, J. Diels, J. Vandeborght, H. Vereecken and J. Feyen. 1998. Analysis of steady-state chloride transport through two homogeneous field soils. *Water Resources Research* 34: 2539–2550.

Marquardt, D.W. 1963. An algorithm for least squares estimation of non-linear parameters. *Journal of Industrial Applied Mathematics* 11: 431–441.

Mishra, S. and J.C. Parker. 1989. Parameter estimation for coupled unsaturated flow and transport. *Water Resources Research* 25: 385–396.

Mualem, Y. 1976. A new model for predicting the hydraulic conductivity of unsaturated porous media. *Water Resource Research* 12: 513–522.

Rahman, S., Y. Chen, K. Buckley and W. Akinremi. 2004. Slurry distribution in soil as influenced by slurry application micro-rate and injection tool type. *Biosystems Engineering* 89: 495–504.

Richard, G.A., L.S. Pereira, D. Raes and M. Smith. 1998. Crop evapotranspiration: Guidelines for computing crop water requirements. Irrigation and drainage paper 56. Rome, Italy: Food and Agriculture Organization of the United Nations (FAO).

Ritsema, C.J. and L.W. Dekker. 1996. Influence of sampling strategy on detecting preferential flow paths in water-repellent sand. *Journal of Hydrology* 177: 33–45.

Schaap, M.G., F.J. Leij and M.Th. van Genuchten. 2001. Rosetta: A computer program for estimating soil hydraulic parameters with hierarchical pedotransfer functions. *Journal of Hydrology* 251: 163–176.

Simunek, J., D. Jacques, J.W. Hopmans, M. Inoue, M. Flury and M.Th. van Genuchten. 2002. Solute transport during variably-saturated flow - inverse methods. In *Methods of Soil Analysis: Part 1. Physical Methods* eds. J.H. Dane and G.C. Topp, 1435–1449, Madison, WI: Soil Science Society of America.

Simunek, J., M. Sejna and M.Th. van Genuchten. 1999. The Hydrus2D software package for simulating two-dimensional movement of water, heat and multiple solutes in variably saturated media, version 2.0. IGWMC-TPS-53. Golden, CO: International Ground Water Modeling Center, Colorado School of Mines.

Snow, V.O., B.E. Clothier, D.R. Scotter and R.E. White. 1994. Solute transport in a layered soil: experiments and modeling using convection-dispersion approach. *Journal of Contaminant Hydrology* 16: 339–358.

Sun, N.Z. and W.W.G. Yeh. 1990. Coupled inverse problems in groundwater modeling: 1. Sensitivity analysis and parameter identification. *Water Resource Research* 26: 2507–2525.

Tsang, Y.W., C.F. Tsang, F.V. Hale and B. Dverstop. 1996. Tracer transport in a stochastic continuum model of fractured media. *Water Resources Research* 32: 3077–3092.

van Genuchten, M.Th. 1980. A closed form equation for predicting the hydraulic conductivity of unsaturated soils. *Soil Science Society of America Journal* 44: 892–898.

Ventrella, D., B.P. Mohanty, J. Simunek, N. Losavio and M.Th. van Genuchten. 2000. Water and chloride transport in a fine-textured soil: Field experiments and modeling. *Soil Science* 165: 624–631.

Xiang, Y., F. Sykes and N.R. Thomson. 1992. A composite L_1 parameter estimator for model fitting in groundwater flow and solute transport simulation. *Water Resources Research* 29: 1661–1673.